Aperiodic neural activity reflects metacontrol

Zhang, C.; Stock, A.K.; Mückschel, M.; Hommel, B.; Beste, C.

OXFORD

Cerebral Cortex, 2023, 1–11
https://doi.org/10.1093/cercor/bhad089
Original Article

Aperiodic neural activity reflects metacontrol

Chenyan Zhang[1], Ann-Kathrin Stock[2], Moritz Mückschel[2], Bernhard Hommel[2,3], Christian Beste[2,3,*]

[1]Cognitive Psychology Unit, Leiden Institute for Brain & Cognition, Institute of Psychology, Leiden University, 2300 RA Leiden, Netherlands,
[2]Cognitive Neurophysiology, Department of Child and Adolescent Psychiatry, Faculty of Medicine, Technische Universität Dresden, 01069 Dresden, Germany,
[3]School of Psychology, Shandong Normal University, 250061 Jinan, China

*Corresponding author: Cognitive Neurophysiology, Department of Child and Adolescent Psychiatry, Faculty of Medicine of the TU Dresden, Schubertstrasse 42, D-01309 Dresden, Germany. Email: christian.beste@uniklinikum-dresden.de

Higher-level cognitive functions are mediated via complex oscillatory activity patterns and its analysis is dominating cognitive neuroscience research. However, besides oscillatory (period) activity, also aperiodic activity constitutes neural dynamics, but its relevance for higher-level cognitive functions is only beginning to be understood. The present study examined whether the broadband EEG aperiodic activity reflects principles of metacontrol. Metacontrol conceptualizes whether it is more useful to engage in more flexible processing of incoming information or to shield cognitive processes from incoming information (persistence-heavy processing). We examined EEG and behavioral data from a sample of $n = 191$ healthy participants performing a Simon Go/NoGo task that can be assumed to induce different metacontrol states (persistence-biased vs. flexibility-biased). Aperiodic activity was estimated using the FOOOF toolbox in the EEG power spectrum. There was a higher aperiodic exponent and offset in NoGo trials compared with Go trials, in incongruent (Go) trials compared with congruent (Go) trials. Thus, aperiodic activity increases during persistence-heavy processing, but decreases during flexibility-heavy processing. These findings link aperiodic features of the EEG signal and concepts describing the dynamics of how cognitive control modes are applied. Therefore, the study substantially extends the importance of aperiodic activity in understanding cognitive functions.

Key words: Aperiodic neural activity; Neural noise; EEG; Cognitive control; Persistence; Flexibility.

Introduction

Higher-level cognitive functions are mediated via complex oscillatory activity patterns (Ward 2003; Fries 2005; Buzsáki 2006; Beste et al. 2023), and the analysis of these pattern has been dominating cognitive neuroscience research using electrophysiological methods (e.g. using the EEG) for decades. Crucially, such EEG power spectra are comprised of two components: the periodic component (also known as neural oscillations) and the aperiodic component (He 2014; Voytek and Knight 2015). Neural oscillations are recurring patterns of brain activity with a particular temporal frequency and have been linked to a wide variety of cognitive processes and behaviors.

The aperiodic component is often described as background activity or "scale-free" broadband activity, which follows a $1/f$-like distribution with decreasing spectral power across increasing frequency (Pritchard 1992; He 2014; Donoghue et al. 2020). This component can be described by a $1/f^x$ function, where f represents the frequency and x reflects an exponent that determines the steepness of the decrease in power across frequencies (Miller et al. 2009; Voytek and Knight 2015; Donoghue et al. 2020). The aperiodic component of the EEG power spectrum is characterized by the aperiodic exponent (x, $1/f$ slope) and aperiodic offset. The aperiodic exponent is analogous to the negative slope of the log-log transformed power spectrum, reflecting the steepness (or slope) of the decay of power across frequencies (Donoghue et al. 2020). The aperiodic offset denotes the broadband shift in power across frequencies.

The aperiodic component was traditionally treated either as noise or a nuisance variable to be neglected or corrected for (Groppe et al. 2013; Gyurkovics et al. 2021). Generally, the topic of "noise" in neural activity and its relevance for human (cognitive) brain function has attracted considerable importance in recent years (Nakao et al. 2019; Wolff et al. 2022; Zhang and Northoff 2022). The neurophysiological origin and functional significance of the aperiodic component of the EEG spectrum are currently not fully understand. However, there is accumulating evidence for a cognitive importance of the aperiodic component, as well as its developmental and clinical relevance (He et al. 2010; Voytek et al. 2015; Huang et al. 2017; Pertermann et al. 2019a; Donoghue et al. 2020; Merkin et al. 2021; Münchau et al. 2021; Ostlund et al. 2021; Wainio-Theberge et al. 2021; Adelhöfer et al. 2021b; Gyurkovics et al. 2022; Hill et al. 2022; Shuffrey et al. 2022; Virtue et al. 2022). Of particular interest, recent studies have shown aperiodic activity to be modulated by the behavioral state (Podvalny et al. 2015), task performance (He et al. 2010), arousal level (Lendner et al. 2020), working memory (Donoghue et al. 2020; Virtue et al. 2022), and cognitive control processes, such as response inhibition (Pertermann et al. 2019b). Recent work showed a steeper $1/f$ slope (i.e. increased exponent) during the controlled inhibition of a prepotent response (Pertermann et al. 2019a, 2019b). More recently, it has been suggested that 1/f slope in EEG signals may serve as a maker of "neural variability," which enables the brain to dynamically adjust its neural activity to meet the demands of a given situation (Waschke et al. 2021b). Both, the findings that $1/f$ activity may reflect a process enabling the brain to dynamically adjust its neural activity to meet the demands of a given situation, and findings underlining the relevance of $1/f$ activity in cognitive control (Pertermann et al. 2019a, 2019b) suggest that $1/f$ activity

Received: December 28, 2022. **Revised:** February 25, 2023. **Accepted:** February 27, 2023

may be relevant for the for the understanding of how the brain dynamically adjust the processing mode/style in higher-level cognitive functions.

The cognitive-control style people prefer or engage in when facing a particular situation has been referred to as "metacontrol" (Hommel 2015). Situations or so-called control dilemmas do not just call for cognitive functions to operate, but to operate in particular ways. For instance, some situations require or call for a persistent, focused control style—like when facing distracting but irrelevant information, while others require or call for a more flexible, open and associative control style—like when acting under uncertainty. The fact that people can deal with both kinds of situations suggests that they can adjust their control style (to some degree) between extreme persistence and extreme flexibility (Goschke 2000; Goschke and Bolte 2014; Hommel and Colzato 2017; Beste et al. 2018). A strong bias toward persistence is assumed to imply strong focus on the current goal and the processing of task-relevant information only, whereas a strong bias toward flexibility should involve a broader focus and openness even to currently task-irrelevant information (Hommel 2015).

The Metacontrol State Model (MSM: Hommel 2015) assumes that cognitive control styles reflect metacontrol states that emerge from (or are represented by) the interplay of functional/neural systems promoting persistence on the one hand and flexibility on the other. A persistence bias is characterized by the increased top-down impact of the current goal and stronger competitions between alternatives, which makes it easier to stick with goal-consistent actions and suppress irrelevant information. In contrast, a flexibility bias is characterized by a reduced impact of the goal and irrelevant alternatives, which facilitates the switch to other options. Interestingly, metacontrol biases not only show systematic individual differences, but also vary with task demands (Hommel and Colzato 2017; Mekern et al. 2019; Zhang et al. 2022). Aperiodic neural activity explains variance in human cognitive control (i.e. response inhibition) (Pertermann et al. 2019a; Pertermann et al. 2019b). If this variance reflects differences in metacontrol states, metacontrol may thus be reflected by aperiodic activity. This will considerably broaden the conceptual relevance of this aspect of neurophysiological activity. This possibility would also fit with considerations that situational noise (i.e. the presence of distracting information) may be an important parameter to adjust metacontrol biases toward more flexibility or persistence (Goschke 2000; Goschke and Bolte 2014; Hommel and Colzato 2017).

Aperiodic activity, as estimated by the slope of the 1/*f* noise function (He et al. 2010; He 2014; Voytek and Knight 2015; Dave et al. 2018) (for critique see Touboul and Destexhe 2017), is determined by the level of neuronal population spiking activity (Voytek and Knight 2015). This activity contributes to local field potentials which constitute large parts of the EEG signal (Katzner et al. 2009; Musall et al. 2014). Synchronized neuronal spiking activity is associated with reduced neuronal noise. In contrast, asynchronous spiking, related to increased neural noise levels, is associated with a flatter slope (Podvalny et al. 2015), of the 1/*f* parameter. Therefore, the 1/*f* parameter (reflecting aperiodic or "noise" activity) may be of relevance when it comes to concepts (such as metacontrol) drawing on internal "noise" as a parameter regulating the system's state shifts more to the flexibility or the persistence. The central hypothesis of the current study is thus that metacontrol states, and their dynamic adjustment to task demands, might be reflected by, and thus associated with different levels of aperiodic neural activity.

We tested this hypothesis by assessing the level of aperiodic neural activity during a cognitive control task that can be assumed to induce different metacontrol states (persistence-biased vs. flexibility-biased). A recently developed spectral parameterization approach [Fitting Oscillations and One Over *f* (FOOOF); Donoghue et al. 2020] was applied to estimate aperiodic activity of EEG signals including aperiodic exponent and offset. We attempted to induce different metacontrol states by means of a Simon Go/NoGo task, which combines a Simon task (Simon 1969) with a Go/NoGo task (Chmielewski and Beste 2017; Chmielewski et al. 2018; Wendiggensen et al. 2022). In the Simon task, participants were required to carry out spatial responses (i.e. left and right) to a non-spatial feature of a stimulus (i.e. letter "A" and "B") presented on the left or right side of the screen. The spatial stimuli are assumed to prime responses in corresponding locations (Simon 1969; Hommel 2011), which should facilitate performance if this response is the correct one (i.e. if it is signaled by the relevant stimulus—so-called congruent conditions) but impair performance if this response is the wrong one (i.e. if the relevant stimulus signals the other response)—the incongruent condition. Hence, participants face more response conflict in incongruent than congruent conditions (Hommel 2011). Overcoming this conflict requires a more persistent control style, supporting stronger focus on the relevant and more neglect of the irrelevant information (Botvinick et al. 2004; Botvinick 2007). Accordingly, we expected that incongruent trials would be associated with a stronger metacontrol bias toward persistence than congruent trials.

This Simon task was combined with a Go/NoGo task, which means that in some trials, participants were to withhold their response. Importantly, for our purposes, Go stimuli were more frequently presented (70% Go trials), which can be expected to result in a prepotent Go response. Biased response probabilities are commonly assumed to reduce top-down control demands for the more frequent response(s) and accordingly increase top-down, goal-driven control demands for the less frequent response(s) (Bokura et al. 2001). Accordingly, we expected the NoGo trials to be associated with a stronger metacontrol bias toward persistence than Go trials. The combination of Simon task and Go/NoGo task yielded four conditions, which should be associated with different metacontrol biases: Whereas (frequent) Go trials and congruent conditions would be more likely to come with a comparatively stronger bias toward metacontrol flexibility, (less frequent) NoGo trials and incongruent trials should come with a comparatively stronger bias toward persistence. Moreover, as the Simon conflict in incongruent Simon trials should enhance inhibitory control, which, in turn, would benefit correct (no) responses in the NoGo condition (for detailed explanation, see Chmielewski and Beste 2017), NoGo congruent trials should come with more persistence-heavy processing (or less flexibility-heavy processing) than NoGo incongruent trials.

Intriguingly, emerging evidence indicates a role of neural activity in the pre-trial period (or between-trial period), which is the time window before the stimuli presentation during inhibitory control (Adelhöfer and Beste 2020; Adelhöfer et al. 2021a; Prochnow et al. 2022; Wendiggensen et al. 2022), as it may reflect a "stage-setting state" that affects subsequent cognitive processes. Therefore, besides the typically used within-trial period (i.e. a time window after stimulus presentation), we also assessed aperiodic activity during the pre-trial period.

Materials and methods

Participants

The present study reanalyzed existing data which were collected for other scientific aims with a cohort of $n = 204$ participants. As 13 participants were identified as outliers, the reported analyses are from $n = 191$ participants (99 females; age 18–40 years; M = 24.93; SD = 4.28). Participants were identified as outliers and excluded from further data analyses if one of the following criteria were met: false alarm rate in NoGo trials higher than 60%, FOOOF spectra fits (R^2) smaller than group mean minus three times standard deviation (SD), and aperiodic exponent or offset values exceeds group mean $\pm 3 \times$ SD. All remaining participants were right-handed with no record of neurological or psychiatric illnesses. The present study was approved by the Psychology Research Ethics Committee of Leiden University and by the TU Dresden. The original study was approved by the Ethics Commission of the TU Dresden, and all participants provided written informed consent for their participation. The study was conducted in accordance with the Declaration of Helsinki.

Task

A combined Simon-Go/NoGo task (Chmielewski and Beste 2017) was employed to assess cognitive control. The different task conditions are illustrated in Fig. 1. Participants were presented with letter stimuli and were instructed to make corresponding responses or no response to a given stimulus. In each trial, a letter "A" or "B" was displayed either in normal font (i.e. "A," "B") or in bold-italics (i.e. "**A**" or "**B**"). A normal font "A" or "B" indicated Go trials in which participants were required to respond as fast as possible, while bold italics "**A**" or "**B**" represented NoGo trials in which responses had to be inhibited. In Go trials, participants were required to press the left "Ctrl" button when the stimulus was an "A" and right "Ctrl" button when it was a "B" regardless of the spatial position of the stimuli. Letter stimuli pseudo-randomly appeared on the left or right side. There were two Go conditions: the congruent Go condition = stimuli were presented on the side of the hand carrying out the response (i.e. "A" on the left side and "B" on the right side); in the incongruent Go condition = stimuli were presented on the opposite side of the hand carrying out the response (i.e. "A" on the right side and "B" on the left side). In NoGo trials, left side '**A**'s and right side '**B**'s indicated congruent NoGo trials, whereas left side '**B**'s and right side '**A**'s represented incongruent NoGo trials.

All stimuli were in white color and presented on a black background. A fixation cross was always displayed in the middle of screen and a white frame box displayed on the left and right sides of the fixation cross was also constantly presented during the task. Each trial started with the letter stimuli presented for 200 ms. In Go trials, participants were asked to respond within 250–1200 ms after stimulus presentation. If no response was made, trials were coded as misses. For NoGo trials, any response within 1,200 ms after stimulus presentation was recorded as a false alarm (i.e. a failure to inhibit the response). Each trial ended after 1700 ms. The inter-trial interval (ITI) was jittered between 1,100 and 1,600 ms. The experiment consisted of 720 trials (70% Go and 30% NoGo trials), of which 50% were congruent trials and 50% were incongruent trials. The test was divided into six equally sized blocks, and trial types were equally distributed across blocks. Before the experiment, each participant completed a practice block of 40 trials.

As behavioral parameter in this Simon Go/NoGo task, we calculated the rate of false alarms (FA, i.e. frequency of responding to a NoGo stimulus), the proportion of correct responses in Go trials (i.e. hit rate) and reaction times (RTs) in correct hits (i.e. hit RT) as behavior parameters of interest.

EEG recording and processing

The data were recorded at the Cognitive Neurophysiology Lab at TU Dresden, Germany. During the Simon-Go/NoGo task, the EEG activity was recorded using QuickAmp and BrainAmp amplifiers (Brain Products GmbH, Gilching, Germany) from 60 equidistantly positioned Ag/AgCl electrodes. All electrodes were referenced to Fpz. The data were recorded at a sampling rate of 500 Hz. Electrode impedances were kept below 5 kΩ. The raw EEG data were preprocessed using the "Automagic" toolbox (Pedroni et al. 2019) and EEGLAB (Delorme and Makeig 2004) on Matlab R2021b (The MathWorks Corp.). First, the raw EEG data were down-sampled to 256 Hz. Afterwards, flat channels were removed, and EEG data were re-referenced to average reference. Subsequently, the PREP preprocessing pipeline (Bigdely-Shamlo et al. 2015) was applied to remove line-noise at 50 Hz and calculate a robust average reference after removing bad channels. The EEGLAB clean_rawdata() pipeline was used to detrend the EEG data using an IIR high-pass filter of 0.5 Hz (slope 80 dB). Flat-line, noisy, and outlier channels were detected and removed. Epochs with extremely strong power (>15 standard deviations relative to calibration data) were reconstructed using Artifact Subspace Reconstruction (burst criterion: 15) (Mullen et al. 2013). Time windows that could not be reconstructed were removed. This is followed by a low-pass filter of 40 Hz (sinc FIR filter; order: 86) (Widmann et al. 2015). EOG artifacts were removed using a subtraction method (Parra et al. 2005). Muscle and remaining eye artifacts were classified and removed by an independent component analysis (ICA)-based Multiple Artifacts Rejection Algorithm (Winkler et al. 2011, 2014). Components containing cardiac artifacts were identified using ICLable (Pion-Tonachini et al. 2019) and removed consecutively. Finally, all removed channels were interpolated using a spherical method.

After preprocessing, the EEG data were segmented and locked to the onset of stimulus. Each segment started at 2,000 ms prior to the stimulus and ended at 2000 ms after the stimulus. Segments were built for Go congruent, Go incongruent, NoGo congruent, and NoGo incongruent conditions, separately. Only correct Go and NoGo trials were analyzed further. An automated artifact rejection procedure was applied in the segmented data to remove trials with residual artifacts (rejection criteria: maximal value difference of 200 μV in a 200-ms interval; activity below 0.5 μV in a 100-ms period). Afterwards, a baseline correction was performed using EEG data from −200 to 0 ms (i.e. stimulus onset).

Parameterization of the spectral data

We used EEG data in a time window from 0 to 1,000 ms after the stimulus presentation as the within-trial period and a time window from −1000 to 0 ms as the pre-trial period. The power spectral density (PSD) for each frequency was calculated using Welch's method (0.25 s Hamming window, 50% overlap) (Welch 1967). The calculation was implemented in Matlab using the "pwelch" function. The PSDs were estimated separately for each participant, electrode, condition, and the pre-trial/within-trial period.

To estimate aperiodic activity, the Python-based FOOOF toolbox (version 1.0.0; https://github.com/fooof-tools/fooof) was applied to parameterize the power spectra by decomposing the aperiodic and periodic components of the signal (for a detailed overview of this approach, see Donoghue et al. 2020) as done in previous work (Adelhöfer et al. 2021b). The FOOOF algorithm conceptualizes the

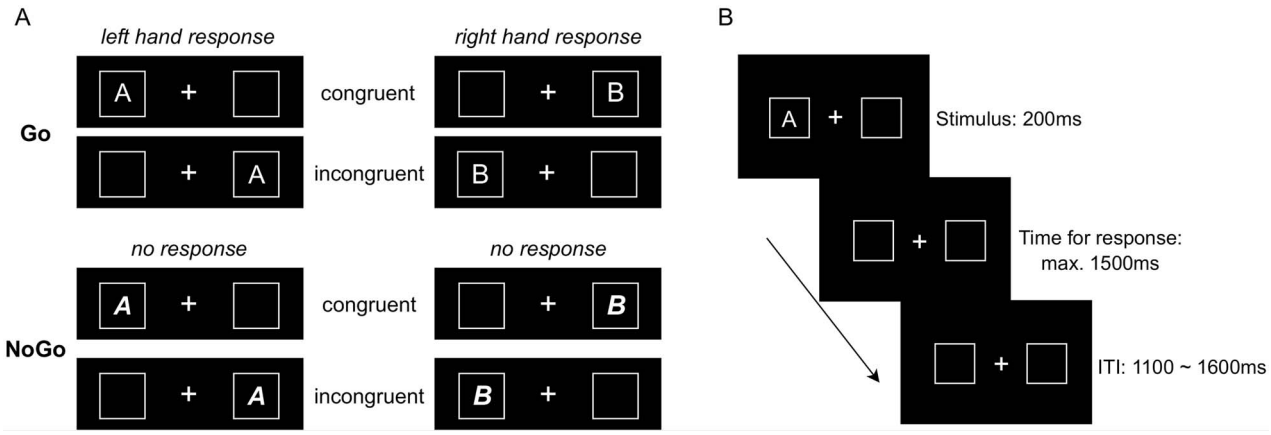

Fig. 1. The Simon Go/NoGo task with all possible stimulus configurations. (A) The Simon Go/NoGo task with all possible stimulus configurations. The upper panel displays stimuli in the go condition. The upper left panel shows stimuli (i.e. "a") which require a left-hand response, whereas the upper right panel shows stimuli (i.e. "B") which require a right-hand response. The lower panel illustrates stimuli (i.e. "**A**" and "**B**") that require no response. (B) The schematic of a trial. Each trial began with the letter stimuli presented for 200 ms. In Go trials, a correct response was recorded if participants responded within 250–1,200 ms after stimulus presentation. In NoGo trials, any response within 1,200 ms after stimulus presentation was recorded as a false alarm. A trial ended after 1,700 ms, followed by the ITI jittered between 1,100 and 1,600 ms.

power spectrum as a linear combination of aperiodic activity [$L(f)$] and periodic (oscillatory) activity [$Gn(f)$]. Precisely, the model of the power spectrum can be written as

$$PSD(f) = L(f) + \sum_{n} G_n(f)$$

where f represents the frequency. The PSD is the linear combination of the aperiodic component, $L(f)$, and n total Gaussians. The aperiodic component is fit as a function across the entire fitted range of the spectrum. The function for the aperiodic component, $L(f)$, is described as

$$L(f) = b - \log[f^x]$$

where b is the aperiodic offset reflecting the broadband power shift, and x is the aperiodic exponent that is equivalent to the slope of the line fitted to the power spectrum in a log-log space. The periodic (oscillatory) components are characterized as frequency regions of power over and above the aperiodic component. Each oscillatory component (also referred to as "peak") is modeled with a Gaussian and characterized by three parameters that define a Gaussian. Each Gaussian fit can be modeled as

$$G_n(f) = a_n \exp\left[-\frac{(f-\mu_n)^2}{2\sigma_n^2}\right]$$

where a_n is the amplitude, μ_n is the center frequency, and σ_n is the bandwidth of each component.

In order to obtain a reliable estimation of the aperiodic component of data, the power spectra data were fit over a broad range of frequency between 1 and 40 Hz, which is consistent with prior studies (Ostlund et al. 2021; Hill et al. 2022) and recommendations in the FOOOF documentation. The FOOOF algorithm used the settings {aperiodic mode = "fixed," peak width limits = [1, 8], maximum number of peaks = 8, minimum peak height = 0.05, default settings otherwise}. The power spectra were fit for each electrode, each participant, each task condition, and each period. The average R^2 of spectral fits for all participants was 0.98 (n = 191).

Aperiodic exponent and offset

The aperiodic exponent and offset were extracted from the aperiodic-only signal for each participant and for each EEG electrode. Due to the absence of priori assumptions regarding the scalp distribution of the aperiodic neural activity, we adopted the "global" exponent and offset in the statistical analysis (Hill et al. 2022). The "global" exponent and offset were obtained by averaging the exponent and offset values across 60 electrodes for each participant. To analyze the scalp distribution of the aperiodic components, we performed an additional cluster-based permutation test where significant results were reached at the global level. The non-parametric cluster-based permutation test was proposed to localize effects in space, frequency, and time while correcting the multiple comparison problem in high-dimensional EEG/MEG data (see Maris and Oostenveld 2007 for details). Here, we applied this approach to identify electrodes that differ between conditions over participants. Clusters were formed based on the adjacency of thresholded sample-level F-values (α = 0.005). The sum of F-values in a cluster was used as the cluster-level statistics. Significant clusters were obtained based on 1,000 Monte Carlo random sampling using the 0.05 significance level.

Statistical analysis

The aperiodic exponent and offset were analyzed using two-way repeated measures ANOVAs. The factor "Go/NoGo" (Go versus NoGo) and factor "congruency" (congruent versus incongruent) were used as within-participants factors. Simple effect analyses were performed where the interaction effect is significant. All post hoc tests were Bonferroni-corrected. Wilcoxon tests were used to evaluate differences in behavioral performance between task conditions, as our behavioral data (i.e. the hit rate and hit RT in Go trials, and false alarm rate in NoGo trials) were not normally distributed. Paired-sample t-tests were employed to test differences in aperiodic activity between the pre-trial and within-trial period. All t-tests are two-tailed. Bayesian statistics were reported for all ANOVAs, Wilcoxon tests, and paired-sample t-tests. In ANOVAs, the inclusion Bayesian factor (BF_{incl}) was calculated to assess the evidence in the data for including a predictor (van den Bergh et al. 2020; van Bergh et al. 2022). For the Wilcoxon test and

Fig. 2. Descriptive statistics for behavioral data. (A) shows the hit rate in go trials; (B) displays the mean RT in go trials; (C) depicts the false alarm rate in NoGo trials. Each violin plot contains a boxplot. The black dot within the box represents the median; the box in the center represents interquartile range; the vertical black line depicts the remaining distribution, except for any data points identified as "outliers" (i.e. those more than 1.5 standard deviations above or below the median).

paired-sample *t*-test, the BF_{10} was used to quantify the evidence supporting the alternative hypothesis over null hypothesis. Statistical analyses were performed using SPSS and JASP packages.

Results

Behavior results

The descriptive results of behavioral data are illustrated in Fig. 2. Wilcoxon tests showed that, within Go trials, the rate of correct responses (hit rate) in the congruent condition (0.96 ± 0.03) was significantly higher than the incongruent condition (0.95 ± 0.05) ($Z = -6.00$, $P < 0.001$; $BF_{10} = 53{,}513.87$). RTs)in the congruent condition (511 ± 81 ms) were significantly faster than in the incongruent condition (529 ± 77 ms) ($Z = -9.76$, $P < 0.001$; $BF_{10} = 5.63 \times 10^6$), indicating a robust Simon effect. The false alarm rate was significantly higher in the congruent NoGo condition (0.13 ± 0.12), as compared with the incongruent NoGo condition (0.10 ± 0.10) ($Z = -8.81$, $P < 0.001$; $BF_{10} = 9.72 \times 10^6$).

Aperiodic exponent and offset results in the pre-trial and within-trial period

Figure 3 shows the PSD in a log-log space at the frequency from 1 Hz to 40 Hz for different experimental conditions in the within-trial period and pre-trial period, separately. PSDs were averaged across electrodes and participants.

In the pre-trial period, two-way repeated measures ANOVAs revealed no significant main effect or interaction effect for either the aperiodic exponent or the aperiodic offset (all $P > 0.05$, $BF_{incl} < 1$).

In the within-trial period, the two-way repeated measures ANOVA for the aperiodic exponent revealed a significant Go/NoGo main effect ($F(1,190) = 37.64$, $P < 0.001$, $\eta_p^2 = 0.17$; $BF_{incl} = 2.09 \times 10^6$). The aperiodic exponent in the NoGo condition (1.15 ± 0.13) was higher than the Go condition (1.14 ± 0.13), thus indicating more aperiodic activity in the NoGo condition than the Go condition. A significant interaction between Go/NoGo and congruency was evident ($F(1,190) = 8.98$, $P = 0.003$, $\eta_p^2 = 0.05$; $BF_{incl} = 13.53$). The simple effect analysis showed that, within Go trials, the aperiodic exponent in the incongruent condition (1.14 ± 0.13) was significantly higher than the congruent condition (1.14 ± 0.13) ($P < 0.001$; $BF_{10} = 193.72$). Within NoGo trials, no significant difference was found in aperiodic exponent between the congruent and incongruent condition ($P > 0.05$; $BF_{10} = 0.04$) (see Fig. 4A and B).

The analysis for the within-trial aperiodic offset showed a significant Go/NoGo main effect ($F(1,190) = 60.56$, $P < 0.001$, $\eta_p^2 = 0.24$; $BF_{incl} = 1.43 \times 10^{10}$). The aperiodic offset in the NoGo condition (0.61 ± 0.22) was higher than the Go condition (0.59 ± 0.21). A significant interaction effect between Go/NoGo and congruency was also found ($F(1,190) = 7.30$, $P = 0.008$, $\eta_p^2 = 0.04$; $BF_{incl} = 5.52$). More precisely, within the Go condition, the aperiodic offset was significantly higher in incongruent trials (0.59 ± 0.21) compared with congruent trials (0.58 ± 0.21) ($P = 0.001$; $BF_{10} = 51.12$). No significant difference was found between congruent and incongruent trials in offset in NoGo condition ($P > 0.05$; $BF_{10} = 0.05$) (see Fig. 4C and D).

Above analyses were based on the aperiodic exponent and offset averaged across all electrodes. To explore the scalp distribution of aperiodic parameters, we performed a cluster-based permutation test to detect electrodes contributing to significant differences between task conditions. The analysis was performed for the within-trial period only, as no difference was identified in the pre-trial period at the "global" level. The scalp topography for aperiodic exponent and offset is shown in Fig. 5. For the aperiodic exponent parameter, the "Go/NoGo × congruency" interaction was evident at FC2, FC3, FC4, Cz, C4, CP2. The significant "Go/NoGo × congruency" interaction effect in the offset parameter was observed at FC1, FC2, Cz, CP2. We found a broad range of electrodes across frontal, central, temporal, posterior, and occipital areas where aperiodic exponent and offset in Go trials were significantly different with them in NoGo trials. Vastly evident differences were observed in frontal-central and posterior regions.

The comparison of aperiodic activity in pre-trial and within-trial period

To test the difference of aperiodic activity between the pre-trial and within-trial time window, we performed paired-sample *t*-tests for the aperiodic exponent and the aperiodic offset separately. Results reflected significantly higher aperiodic activity in the within-trial period compared with the pre-trial period in all task conditions (all $P < 0.001$, $BF_{10} \geq 2.41 \times 10^{64}$) (see Table 1), indicating increased aperiodic neural activity for task execution (i.e. in the within-trial period).

Discussion

The main aim of the present study was to test whether the broadband aperiodic activity in the EEG power spectrum is associated with demand-specific biases of metacontrol toward persistence or flexibility. To achieve this, we assessed the aperiodic activity in the EEG power spectrum during a Simon Go/NoGo task in the pre-trial period and within-trial period, separately. Using the cluster-based permutation test, we then examined the scalp distribution for aperiodic exponent and offset parameters. Several key findings

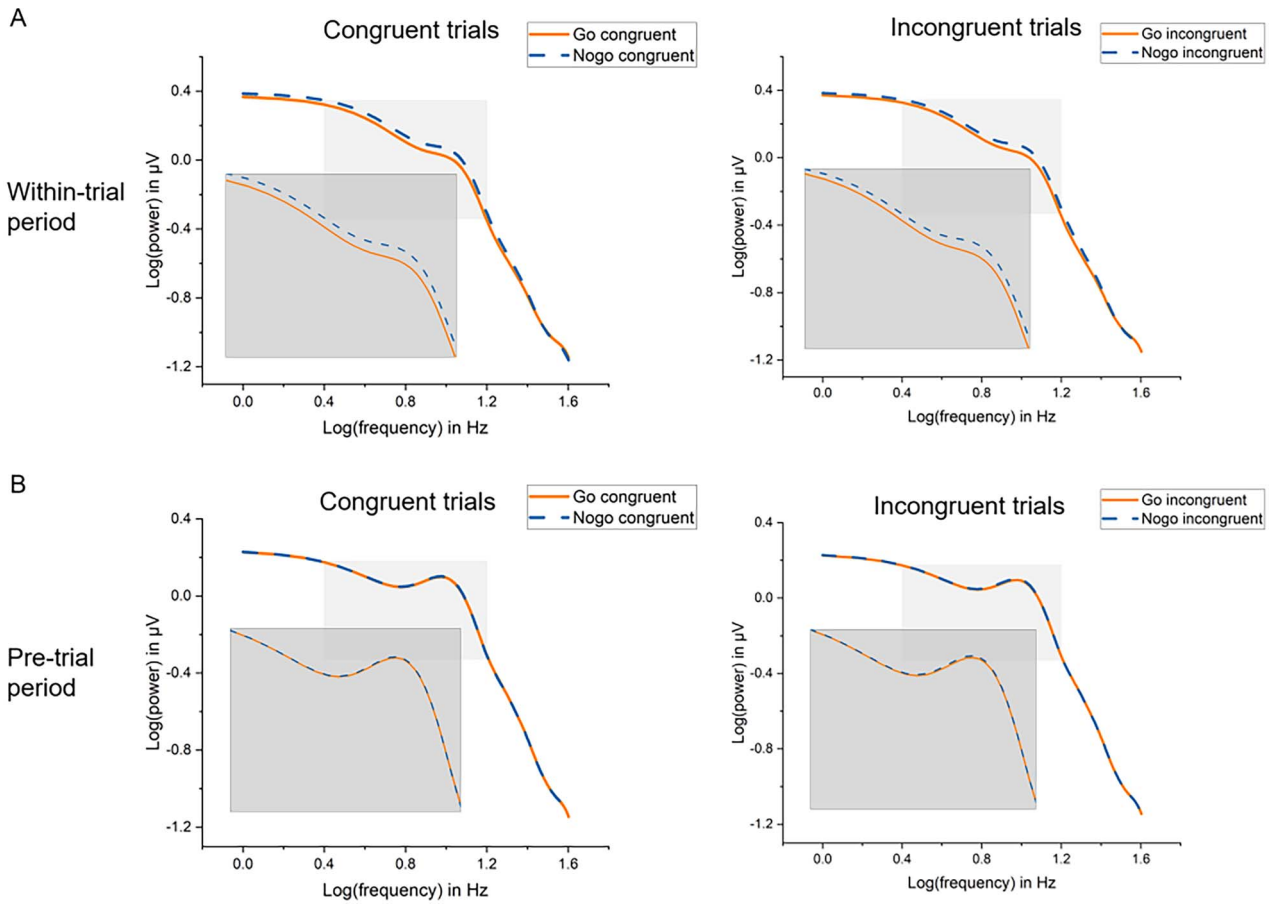

Fig. 3. Log-log transformed power spectral densities averaged across electrodes and participants. (A) shows PSDs in the within-trial period; (B) displays PSDs in the pre-trial period. The left figure showed PSDs for congruent trials, and the right figure displayed PSDs for incongruent trials.

emerged from this study: First, in the within-trial period, the aperiodic exponent and offset were higher in the NoGo condition than the Go condition. The aperiodic activity in incongruent trials was higher than congruent trials in the Go condition; however, the difference failed to reach significance in the NoGo condition. In contrast, in the pre-trial period, no significant difference was detected for aperiodic activity between experimental conditions. Second, we found significant Go/NoGo effects in the aperiodic exponent and offset across a number of electrodes over the scalp, and Go/NoGo × congruency effects in several frontal and central electrodes. In addition, we observed increased aperiodic activity across task conditions in the within-trial period, as compared with the pre-trial period.

Importantly, our findings suggest that aperiodic activity measured in the EEG power spectrum reflects metacontrol states or, more specifically, dynamic adjustments of metacontrol states to task demands: More concretely, in the within-trial period, we observed increased aperiodic exponent and offset values in the NoGo condition than in the Go condition. As explained above, the infrequent NoGo trials should have induced more response conflict, which would need to be overcome with a stronger persistence bias in metacontrol (Hommel 2015). In contrast, in Go trials, the stimulus conditions unequivocally support the correct response, so that participants can afford a more flexible metacontrol state. Another indication that metacontrol is reflected in aperiodic activity is that, in the Go condition, the aperiodic exponent and offset values were higher in (persistence-heavy) incongruent trials than in (flexibility-friendly) congruent trials. As discussed above, incongruent trials can be assumed to induce more response conflict. Given that both responses are legal responses in the task, this conflict can only be overcome by relying on goal-information, which, in turn, implies a stronger metacontrol bias toward persistence. Taken together, these findings suggest that aperiodic activity increases during persistence-heavy processing, but decreases during flexibility-heavy processing.

Several studies have demonstrated that aperiodic activity is modulated by the behavioral state (Podvalny et al. 2015), task performance (He et al. 2010) and arousal level (Lendner et al. 2020). A recent study by Pertermann et al. (2019a, b), who recorded EEG activity during the motor response inhibition task, found a steeper "1/*f* slope" (i.e. higher aperiodic exponent) when inhibiting a prepotent response. Our results extend previous findings by demonstrating that aperiodic activity reflects the demand-specific metacontrol state, with increased values during persistence-heavy processing and reduced values during flexibility-heavy processing. It is also noteworthy that main or interaction effects did not reach significance in the pre-trial period (i.e. before the stimulus presentation). This observation may suggest that the modulation of aperiodic activity is reactive and stimulus-induced—which would fit with the counter-intuitive idea that control operations may be driven by the environment (Waszak et al. 2003; Dignath et al. 2019). Based on MEG data, recent research has shown that aperiodic activity demonstrates less significant task-related changes than oscillatory activity, indicating a more stable aspect of brain activity (Wainio-Theberge et al. 2022). Our results expand upon

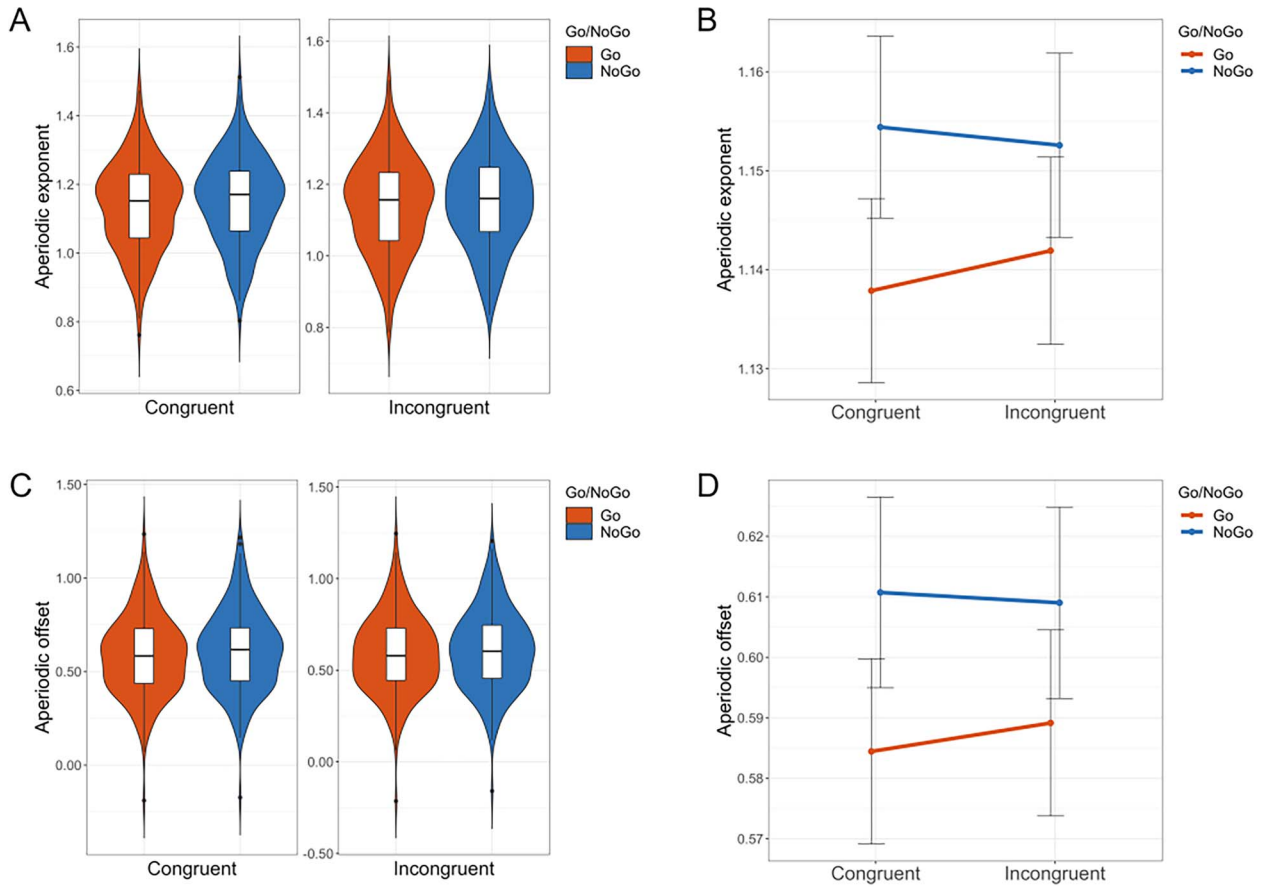

Fig. 4. Descriptive results for the within-trial aperiodic exponent and offset in different Simon Go/NoGo conditions. (A) and (B) show the violin plot and line plot for the aperiodic exponent in different task conditions; (C) and (D) reveal the violin plot and line plot for the aperiodic offset in different experimental conditions. Each violin plot contains a boxplot. The horizonal line within the box represents the median; the box in the center represents interquartile range; the vertical black line depicts the remaining distribution, except for any data points identified as "outliers" (i.e. those more than 1.5 standard deviations above or below the median). In line plots, error bars represent the standard error of the mean.

prior findings and indicate that, while aperiodic activity can serve as a stable background for neural activity, it also demonstrates the capacity to adapt to changing cognitive demands. Furthermore, the observation of higher aperiodic activity in the within-trial period than pre-trial period indicates a tight connection between aperiodic activity and metacontrol states, in keeping with recent findings that the steepness of 1/*f* activity increases after auditory stimulation (Gyurkovics et al. 2022).

Although the precise neurophysiological and cognitive mechanisms underlying aperiodic activity remain under discussion, several potential explanations for aperiodic exponent in EEG signals have been proposed. The "neural noise" account assumes that aperiodic exponent in EEG signals is a measure of the level of noise in the underlying neural circuits (He et al. 2010; Voytek and Knight 2015; Voytek et al. 2015; Gao 2016; Dave et al. 2018). Synchronized neural spiking activity results in a steeper 1/*f* slope and is associated with an increased signal-to-noise ratio (SNR) in the nervous system, whereas asynchronous spiking activity gives rise to a flatter 1/*f* slope and decreased SNR (Podvalny et al. 2015; Voytek and Knight 2015; Voytek et al. 2015). The neural noise account of aperiodic activity has been extensively employed to gain a better understanding of clinical phenomena, such as schizophrenia (Wolff et al. 2022), Tourette syndrome (Münchau et al. 2021; Adelhöfer et al. 2021b), ADHD (Pertermann et al. 2019a; Ostlund et al. 2021), and age-related cognitive decline (Voytek et al. 2015; Dave et al. 2018). Recently, researchers have considered that 1/*f* slope in EEG signals may serve as a maker of "neural variability," which enables the brain to dynamically adjust its neural activity to meet the demands of a given task or situation (Waschke et al. 2021b). Hence, our findings may indicate that different metacontrol states manifest in altered levels of neural variability, with decreased neural noise/variability during persistence-heavy and increased neural noise/variability during flexibility-heavy processing.

The potential mechanisms underlying the link between aperiodic activity and metacontrol is not yet fully understood. One possible account is that neural variability may be related to dynamics of cortical network states, which could be associated with the representation of goal- and task-related information (Tsujimoto et al. 2008; Deco et al. 2009; Armbruster-Gençet al. 2016; Nogueira et al. 2018). In persistence-heavy processing, the system needs to maintain stable representation of task goals to focus on task-relevant stimuli and ignore task-irrelevant stimuli (Hommel 2015). The sustained representation of task goals may require fewer transitions between cortical network states, reflected by lower neural variability (Durstewitz and Seamans 2008; Tsujimoto et al. 2008; Armbruster-Gençet al. 2016). Therefore, lower aperiodic activity may be associated with more stable cortical network states and sustained representations of the task goal. However, in flexibility-heavy processing, the system is less bounded by the task goal and sensitive to task-irrelevant stimuli (Hommel 2015). This may require/result in

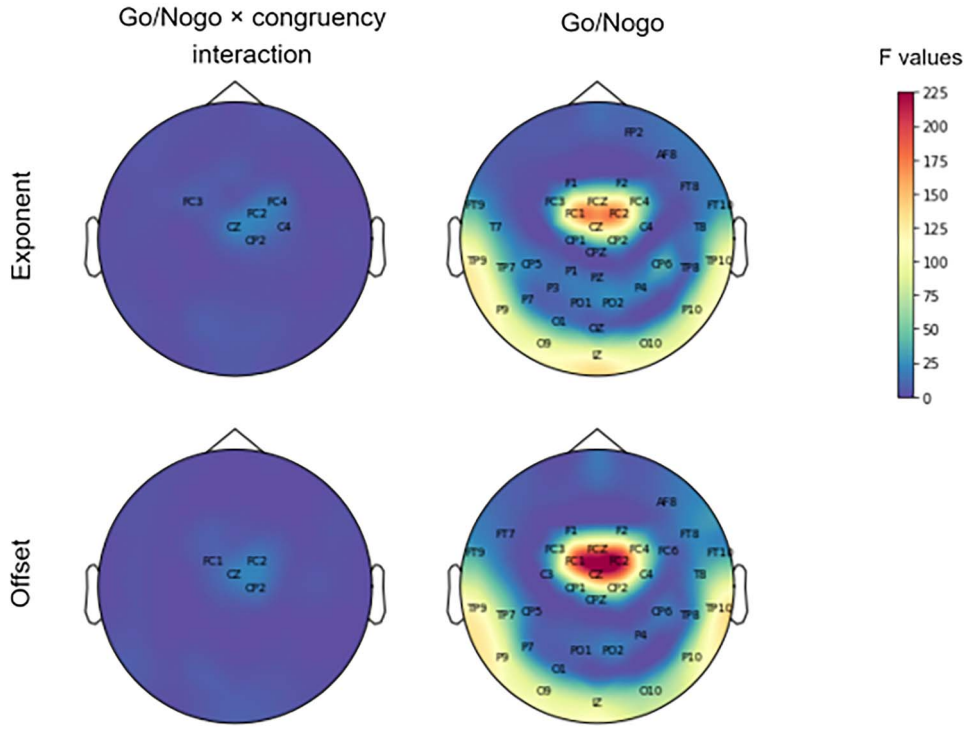

Fig. 5. Scalp distributions of the aperiodic exponent and offset in the within-trial period. Scalp topographies in the upper row show electrode sites with significant "Go/NoGo × congruency" interaction effect (the upper left figure) and Go/NoGo main effect (the upper right figure) in the aperiodic exponent. Scalp topographies in the lower row show electrode sites with significant "Go/NoGo × congruency" interaction effect (the lower left graph) and Go/NoGo effect (the lower right graph) in the aperiodic offset. Labels are shown for significant clusters of electrodes. The colors denote cluster-level summed F-values.

more frequent and easier transitions between cortical network states (Durstewitz and Seamans 2008; Tsujimoto et al. 2008; Armbruster-Gençet al. 2016). Thus, higher neural variability may be associated with easier switches between cortical network states and unstable representations of goal-information. However, this interpretation is currently speculative and requires further research in the future.

In a broader sense, the link between neural noise/aperiodic activity and metacontrol is consistent with previous fMRI findings showing that higher levels of brain variability (i.e. high brain noise) facilitate cognitive flexibility, but impair cognitive stability (Armbruster-Gençet al. 2016). Recent work found that higher levels of resting-state fMRI signal variability are associated with increased flexibility bias of metacontrol (or decreased persistence bias of metacontrol), which also points to an association between neural "noise" and individual metacontrol policies (Zhang et al. 2022). The present findings provide evidence for an interesting connection between neural noise in terms of EEG signal and cognitive metacontrol states.

Moreover, physiological evidence has shown that the balance between excitation and inhibition (E/I) can be estimated from the exponent of EEG power spectrum (Gao et al. 2017; Lombardi et al. 2017). A flatter exponent is assumed to be driven by an increased E/I ratio, whereas a steeper exponent is assumed to be induced by a decreased E/I ratio (Gao et al. 2017; Lombardi et al. 2017). The association between E/I balance and aperiodic activity has been implicated in several studies. For example, Lendner and colleagues (Lendner et al. 2020) discovered that aperiodic exponent can distinguish arousal levels, and higher values found in REM sleep than NREM sleep, and higher values in NREM sleep than during wakefulness. These findings align with in vivo calcium imaging evidence in mice that indicates a shift toward predominant inhibition in cortical networks during REM sleep (Niethard et al. 2016). More recently, a study revealed that aperiodic exponent increased under propofol anesthesia (which results in a relative increase of inhibition), and decreased under ketamine anesthesia (which results in a relative increase of excitation) (Waschke et al. 2021a). The present findings may indicate a decreased E/I ratio during persistence-heavy processing whereas an increased E/I ratio during flexibility-heavy processing. Our results suggest that the state of metacontrol might be associated with a shift toward increased inhibitory tone or toward increased excitatory tone within neural circuits. Even though the aperiodic exponent has been demonstrated to approximate E/I balance (Gao et al. 2017; Lombardi et al. 2017), evidence for joint changes between E/I balance, aperiodic variability, and behavior is still lacking.

Future work may test whether control-related changes in aperiodic activity affect behavior in a direct or indirect manner. The scalp distribution results indicate that the difference of aperiodic activity between the Go and NoGo condition is relatively global, given that a broad range of electrodes on the scalp showed significant Go/NoGo effect for both exponent and offset. In contrast, only a few electrodes in the frontal and central scalp contribute to the congruency effect in the Go condition, indicating a region-specific congruency effect. The finding that aperiodic offset reflects metacontrol states also warrants further investigation. Evidence from humans and macaques demonstrated that broadband power shifts are positively correlated to neuronal population spiking (Manning et al. 2009; Ray and Maunsell 2011). Thus, our present observation of an enlargement in aperiodic offset during persistence-heavy processing and a reduction during flexibility-heavy processing could be tentatively interpreted to reflect a control-state dependent changes in the spiking rates of

Table 1. Comparisons of aperiodic exponent and offset between the pre-trial and within-trial period.

		Exponent					Offset				
		Pre-trial	Within-trial	$t(1, 190)$	P	BF_{10}	Pre-trial	Within-trial	$t(1, 190)$	P	BF_{10}
Conditions	Go congruent	1.03 ± 0.13	1.14 ± 0.13	31.36	<0.001	4.86×10^{73}	0.45 ± 0.21	0.58 ± 0.21	27.3	<0.001	2.40×10^{64}
	Go incongruent	1.03 ± 0.13	1.14 ± 0.13	32.47	<0.001	1.19×10^{76}	0.45 ± 0.21	0.59 ± 0.21	28.54	<0.001	2.03×10^{67}
	NoGo congruent	1.04 ± 0.13	1.15 ± 0.13	30.34	<0.001	2.57×10^{71}	0.45 ± 0.21	0.61 ± 0.22	27.32	<0.001	2.55×10^{64}
	NoGo incongruent	1.03 ± 0.13	1.15 ± 0.13	30.82	<0.001	2.98×10^{72}	0.44 ± 0.21	0.61 ± 0.22	28.38	<0.001	8.79×10^{66}

cortical neurons. The current study opens a window on the role of aperiodic activity in metacontrol, but the precise mechanisms underlying this association remain to be determined.

Acknowledgments

We thank all participants.

CRediT author statement

Chenyan Zhang (Conceptualization, Formal analysis, Funding acquisition, Methodology, Visualization, Writing—original draft, Writing—review and editing), Ann-Kathrin Stock (Data curation, Funding acquisition, Investigation, Project administration, Resources, Writing—review and editing), Moritz Mückschel (Data curation, Methodology, Project administration, Resources, Software, Writing—review and editing), Bernhard Hommel (Conceptualization, Funding acquisition, Resources, Supervision, Validation, Writing—original draft, Writing—review and editing), Christian Beste (Conceptualization, Funding acquisition, Methodology, Project administration, Resources, Software, Supervision, Validation, Writing—original draft, Writing—review and editing).

Funding

Province of Shandong, China (100 Double Talent Grant to C.B. and B.H); Deutsche Forschungsgemeinschaft (DFG) (SFB 940 and SFB TRR 265 to C.B. and A.K.S.); Chinese Scholarship Council (201806990039 to C.Z.).

Conflict of interest statement: None declared.

Data availability

All data can be obtained from the corresponding author upon reasonable request.

References

Adelhöfer N, Beste C. Pre-trial theta band activity in the ventromedial prefrontal cortex correlates with inhibition-related theta band activity in the right inferior frontal cortex. *NeuroImage*. 2020:219:117052.

Adelhöfer N, Bluschke A, Roessner V, Beste C. The dynamics of theta-related pro-active control and response inhibition processes in AD(H)D. *NeuroImage Clin*. 2021a:30:102609.

Adelhöfer N, Paulus T, Mückschel M, Bäumer T, Bluschke A, Takacs A, Tóth-Fáber E, Tárnok Z, Roessner V, Weissbach A, et al. Increased scale-free and aperiodic neural activity during sensorimotor integration-a novel facet in Tourette syndrome. *Brain Commun*. 2021b:3:fcab250.

Armbruster-Genç DJN, Ueltzhöffer K, Fiebach CJ. Brain signal variability differentially affects cognitive flexibility and cognitive stability. *J Neurosci*. 2016:36:3978–3987.

Beste C, Moll CKE, Pötter-Nerger M, Münchau A. Striatal microstructure and its relevance for cognitive control. *Trends Cogn Sci*. 2018:22:747–751.

Beste C, Münchau A, Frings C. Towards a systematization of brain oscillatory activity in actions. *Commun Biol*. 2023:6:137.

Bigdely-Shamlo N, Mullen T, Kothe C, Su KM, Robbins KA. The PREP pipeline: standardized preprocessing for large-scale EEG analysis. *Front Neuroinform*. 2015:9:1–19.

Bokura H, Yamaguchi S, Kobayashi S. Electrophysiological correlates for response inhibition in a Go/NoGo task. *Clin Neurophysiol*. 2001:112:2224–2232.

Botvinick MM. Conflict monitoring and decision making: reconciling two perspectives on anterior cingulate function. *Cogn Affect Behav Neurosci*. 2007:7:356–366.

Botvinick MM, Cohen JD, Carter CS. Conflict monitoring and anterior cingulate cortex: an update. *Trends Cogn Sci*. 2004:8:539–546.

Buzsáki G. *Rhythms of the brain*. Oxford University Press; 2006.

Chmielewski WX, Beste C. Testing interactive effects of automatic and conflict control processes during response inhibition – a system neurophysiological study. *NeuroImage*. 2017:146:1149–1156.

Chmielewski WX, Mückschel M, Beste C. Response selection codes in neurophysiological data predict conjoint effects of controlled and automatic processes during response inhibition. *Hum Brain Mapp*. 2018:39:1839–1849.

Dave S, Brothers TA, Swaab TY. 1/f neural noise and electrophysiological indices of contextual prediction in aging. *Brain Res*. 2018:1691:34–43.

Deco G, Rolls ET, Romo R. Stochastic dynamics as a principle of brain function. *Prog Neurobiol*. 2009:88:1–16.

Delorme A, Makeig S. EEGLAB: an open source toolbox for analysis of single-trial EEG dynamics including independent component analysis. *J Neurosci Methods*. 2004:134:9–21.

Dignath D, Johannsen L, Hommel B, Kiesel A. Reconciling cognitive-control and episodic-retrieval accounts of sequential conflict modulation: binding of control-states into event-files. *J Exp Psychol Hum Percept Perform*. 2019:45:1265–1270.

Donoghue T, Haller M, Peterson EJ, Varma P, Sebastian P, Gao R, Noto T, Lara AH, Wallis JD, Knight RT, et al. Parameterizing

neural power spectra into periodic and aperiodic components. *Nat Neurosci*. 2020:23:1655–1665.

Durstewitz D, Seamans JK. The dual-state theory of prefrontal cortex dopamine function with relevance to catechol-o-methyltransferase genotypes and schizophrenia. *Biol Psychiatry*. 2008:64:739–749.

Fries P. A mechanism for cognitive dynamics: neuronal communication through neuronal coherence. *Trends Cogn Sci*. 2005:9:474–480.

Gao R. Interpreting the electrophysiological power spectrum. *J Neurophysiol*. 2016:115:628–630.

Gao R, Peterson EJ, Voytek B. Inferring synaptic excitation/inhibition balance from field potentials. *NeuroImage*. 2017:158:70–78.

Goschke T. Intentional reconfiguration and involuntary persistence in task set switching. In: Monsell S, Driver J, editors. *Attention and performance*. MIT Press; 2000. pp. 331–355.

Goschke T, Bolte A. Emotional modulation of control dilemmas: the role of positive affect, reward, and dopamine in cognitive stability and flexibility. *Neuropsychologia*. 2014:62:403–423.

Groppe DM, Bickel S, Keller CJ, Jain SK, Hwang ST, Harden C, Mehta AD. Dominant frequencies of resting human brain activity as measured by the electrocorticogram. *NeuroImage*. 2013:79:223–233.

Gyurkovics M, Clements GM, Low KA, Fabiani M, Gratton G. The impact of 1/f activity and baseline correction on the results and interpretation of time-frequency analyses of EEG/MEG data: a cautionary tale. *NeuroImage*. 2021:237:118192.

Gyurkovics M, Clements GM, Low KA, Fabiani M, Gratton G. Stimulus-induced changes in 1/f-like background activity in EEG. *J Neurosci*. 2022:42:7144–7151.

He BJ. Scale-free brain activity: past, present, and future. *Trends Cogn Sci*. 2014:18:480–487.

He BJ, Zempel JM, Snyder AZ, Raichle ME. The temporal structures and functional significance of scale-free brain activity. *Neuron*. 2010:66:353–369.

Hill AT, Clark GM, Bigelow FJ, Lum JAG, Enticott PG. Periodic and aperiodic neural activity displays age-dependent changes across early-to-middle childhood. *Dev Cogn Neurosci*. 2022:54:101076.

Hommel B. The Simon effect as tool and heuristic. *Acta Psychol*. 2011:136:189–202.

Hommel B. Between persistence and flexibility: the Yin and Yang of action control. *Adv Motiv Sci*. 2015:2:33–67.

Hommel B, Colzato LS. The social transmission of metacontrol policies: mechanisms underlying the interpersonal transfer of persistence and flexibility. *Neurosci Biobehav Rev*. 2017:81:43–58.

Huang Z, Zhang J, Longtin A, Dumont G, Duncan NW, Pokorny J, Qin P, Dai R, Ferri F, Weng X, et al. Is there a nonadditive interaction between spontaneous and evoked activity? Phase-dependence and its relation to the temporal structure of scale-free brain activity. *Cereb Cortex*. 2017:27:1037–1059.

Katzner S, Nauhaus I, Benucci A, Bonin V, Ringach DL, Carandini M. Local origin of field potentials in visual cortex. *Neuron*. 2009:61:35–41.

Lendner JD, Helfrich RF, Mander BA, Romundstad L, Lin JJ, Walker MP, Larsson PG, Knight RT. An electrophysiological marker of arousal level in humans. *eLife*. 2020:9:e55092.

Lombardi F, Herrmann HJ, de Arcangelis L. Balance of excitation and inhibition determines 1/f power spectrum in neuronal networks. *Chaos Interdiscip J Nonlinear Sci*. 2017:27:047402.

Manning JR, Jacobs J, Fried I, Kahana MJ. Broadband shifts in local field potential power spectra are correlated with single-neuron spiking in humans. *J Neurosci*. 2009:29:13613–13620.

Maris E, Oostenveld R. Nonparametric statistical testing of EEG- and MEG-data. *J Neurosci Methods*. 2007:164:177–190.

Mekern VN, Sjoerds Z, Hommel B. How metacontrol biases and adaptivity impact performance in cognitive search tasks. *Cognition*. 2019:182:251–259.

Merkin A, Sghirripa S, Graetz L, Smith AE, Hordacre B, Harris R, Pitcher J, Semmler J, Rogasch NC, Goldsworthy M. Age differences in aperiodic neural activity measured with resting EEG. 2021. https://doi.org/10.1101/2021.08.31.458328.

Miller KJ, Sorensen LB, Ojemann JG, den Nijs M. Power-law scaling in the brain surface electric potential. *PLoS Comput Biol*. 2009:5:e1000609.

Mullen T, Kothe C, Chi YM, Ojeda A, Kerth T, Makeig S, Cauwenberghs G, Jung T-P. 2013. Real-time modeling and 3D visualization of source dynamics and connectivity using wearable EEG. In: *2013 35th Annual International Conference of the IEEE Engineering in Medicine and Biology Society (EMBC)*. p. 2184–2187.

Münchau A, Colzato LS, AghajaniAfjedi A, Beste C. A neural noise account of Gilles de la Tourette syndrome. *NeuroImage Clin*. 2021:30:102654.

Musall S, von Pföstl V, Rauch A, Logothetis NK, Whittingstall K. Effects of neural synchrony on surface EEG. *Cereb Cortex*. 2014:24:1045–1053.

Nakao T, Miyagi M, Hiramoto R, Wolff A, Gomez-Pilar J, Miyatani M, Northoff G. From neuronal to psychological noise – long-range temporal correlations in EEG intrinsic activity reduce noise in internally-guided decision making. *NeuroImage*. 2019:201:116015.

Niethard N, Hasegawa M, Itokazu T, Oyanedel CN, Born J, Sato TR. Sleep-stage-specific regulation of cortical excitation and inhibition. *Curr Biol*. 2016:26:2739–2749.

Nogueira R, Lawrie S, Moreno-Bote R. Neuronal variability as a proxy for network state. *Trends Neurosci*. 2018:41:170–173.

Ostlund BD, Alperin BR, Drew T, Karalunas SL. Behavioral and cognitive correlates of the aperiodic (1/f-like) exponent of the EEG power spectrum in adolescents with and without ADHD. *Dev Cogn Neurosci*. 2021:48:100931.

Parra LC, Spence CD, Gerson AD, Sajda P. Recipes for the linear analysis of EEG. *NeuroImage*. 2005:28:326–341.

Pedroni A, Bahreini A, Langer N. Automagic: standardized preprocessing of big EEG data. *NeuroImage*. 2019:200:460–473.

Pertermann M, Bluschke A, Roessner V, Beste C. The modulation of neural noise underlies the effectiveness of methylphenidate treatment in attention-deficit/hyperactivity disorder. *Biol Psychiatry Cogn Neurosci Neuroimaging*. 2019a:4(8):743–750.

Pertermann M, Mückschel M, Adelhöfer N, Ziemssen T, Beste C. On the interrelation of 1/f neural noise and norepinephrine system activity during motor response inhibition. *J Neurophysiol*. 2019b:121:1633–1643.

Pion-Tonachini L, Kreutz-Delgado K, Makeig S. The ICLabel dataset of electroencephalographic (EEG) independent component (IC) features. *Data Brief*. 2019:25:104101.

Podvalny E, Noy N, Harel M, Bickel S, Chechik G, Schroeder CE, Mehta AD, Tsodyks M, Malach R. A unifying principle underlying the extracellular field potential spectral responses in the human cortex. *J Neurophysiol*. 2015:114:505–519.

Pritchard WS. The brain in fractal time: 1/F-like power Spectrum scaling of the human electroencephalogram. *Int J Neurosci*. 1992:66:119–129.

Prochnow A, Wendiggensen P, Eggert E, Münchau A, Beste C. Pre-trial fronto-occipital electrophysiological connectivity affects perception–action integration in response inhibition. *Cortex*. 2022:152:122–135.

Ray S, Maunsell JHR. Different origins of gamma rhythm and high-gamma activity in macaque visual cortex. *PLoS Biol*. 2011:9:e1000610.

Shuffrey LC, Pini N, Potter M, Springer P, Lucchini M, Rayport Y, Sania A, Firestein M, Brink L, Isler JR, et al. Aperiodic electrophysiological activity in preterm infants is linked to subsequent autism risk. *Dev Psychobiol*. 2022:64:e22271.

Simon JR. Reactions toward the source of stimulation. *J Exp Psychol*. 1969:81:174–176.

Touboul J, Destexhe A. Power-law statistics and universal scaling in the absence of criticality. *Phys Rev E*. 2017:95:012413. https://doi.org/10.1103/PhysRevE.95.012413.

Tsujimoto S, Genovesio A, Wise SP. Transient neuronal correlations underlying goal selection and maintenance in prefrontal cortex. *Cereb Cortex*. 2008:18:2748–2761.

van den Bergh D, van Doorn J, Marsman M, Draws T, van Kesteren E-J, Derks K, Dablander F, Gronau QF, Kucharský Š, Gupta ARKN, et al. A tutorial on conducting and interpreting a Bayesian ANOVA in JASP. *LAnnee Psychol*. 2020:120:73–96.

van den Bergh D, Wagenmakers E-J, Aust F. Bayesian repeated-measures ANOVA: an updated methodology implemented in JASP. 2022. https://doi.org/10.31234/osf.io/fb8zn.

Virtue-Griffiths S, Fornito A, Thompson S, Biabani M, Tiego J, Thapa T, Rogasch NC. Task-related changes in aperiodic activity are related to visual working memory capacity independent of event-related potentials and alpha oscillations. 2022. https://doi.org/10.1101/2022.01.18.476852.

Voytek B, Knight RT. Dynamic network communication as a unifying neural basis for cognition, development, aging, and disease. *Biol Psychiatry*. 2015:77:1089–1097.

Voytek B, Kramer MA, Case J, Lepage KQ, Tempesta ZR, Knight RT, Gazzaley A. Age-related changes in 1/f neural electrophysiological noise. *J Neurosci*. 2015:35:13257–13265.

Wainio-Theberge S, Wolff A, Gomez-Pilar J, Zhang J, Northoff G. Variability and task-responsiveness of electrophysiological dynamics: scale-free stability and oscillatory flexibility. *NeuroImage*. 2022:256:119245.

Wainio-Theberge S, Wolff A, Northoff G. Dynamic relationships between spontaneous and evoked electrophysiological activity. *Commun Biol*. 2021:4:741.

Ward LM. Synchronous neural oscillations and cognitive processes. *Trends Cogn Sci*. 2003:7:553–559.

Waschke L, Donoghue T, Fiedler L, Smith S, Garrett DD, Voytek B, Obleser J. Modality-specific tracking of attention and sensory statistics in the human electrophysiological spectral exponent. *eLife*. 2021a:10:e70068.

Waschke L, Kloosterman NA, Obleser J, Garrett DD. Behavior needs neural variability. *Neuron*. 2021b:109:751–766.

Waszak F, Hommel B, Allport A. Task-switching and long-term priming: role of episodic stimulus–task bindings in task-shift costs. *Cogn Psychol*. 2003:46:361–413.

Welch P. The use of fast Fourier transform for the estimation of power spectra: a method based on time averaging over short, modified periodograms. *IEEE Trans Audio Electroacoustics*. 1967:15:70–73.

Wendiggensen P, Ghin F, Koyun AH, Stock A-K, Beste C. Pretrial theta band activity affects context-dependent modulation of response inhibition. *J Cogn Neurosci*. 2022:34:605–617.

Widmann A, Schröger E, Maess B. Digital filter design for electrophysiological data – a practical approach. *J Neurosci Methods*. 2015:250:34–46.

Winkler I, Brandl S, Horn F, Waldburger E, Allefeld C, Tangermann M. Robust artifactual independent component classification for BCI practitioners. *J Neural Eng*. 2014:11:035013.

Winkler I, Haufe S, Tangermann M. Automatic classification of artifactual ICA-components for artifact removal in EEG signals. *Behav Brain Funct*. 2011:7:30.

Wolff A, Gomez-Pilar J, Zhang J, Choueiry J, de la Salle S, Knott V, Northoff G. It's in the timing: reduced temporal precision in neural activity of schizophrenia. *Cereb Cortex*. 2022:32:3441–3456.

Zhang C, Beste C, Prochazkova L, Wang K, Speer SPH, Smidts A, Boksem MAS, Hommel B. Resting-state BOLD signal variability is associated with individual differences in metacontrol. *Sci Rep*. 2022:12:18425.

Zhang J, Northoff G. Beyond noise to function: reframing the global brain activity and its dynamic topography. *Commun Biol*. 2022:5:1350.